

On the Control Design of Half Humanoid for Space Applications

Sangeetha G.R.

AI and Space Robotics Division
IISU/ISRO

Thiruvananthapuram, India

Harikumar Ganesan

AI and Space Robotics Division
IISU/ISRO

Thiruvananthapuram, India

Durairaj R.

AI and Space Robotics Division
IISU/ISRO

Thiruvananthapuram, India

Abstract—The paper presents the control architecture, controller modes, gain tuning and micro-gravity testing and stability analysis of 6 DOF robotic arm of Half Humanoid designed for space applications. A decentralised control architecture is followed with final execution effected through joint level position control loops. Conventional methods for gain tuning using step and frequency response analysis methods have been adopted, albeit in micro-gravity(micro-g) simulated configurations of the arm, sufficiency of which is established. The stability of the joint loops are ensured by the relative stability margins and hardware test results are presented.

Index Terms—Robotic arm, micro-gravity, stability analysis, zero-g orientation, controller tuning

I. INTRODUCTION

Robotic assistants can serve as precursors for human missions and set stage for human arrival. Among the different types of robots such as rovers, humanoids, free-flyers and manipulators, humanoids are particularly suitable for performing in human engineered environments. There has been many successful demonstrations of Humanoids working in the space environment such as the Robonaut 2 by NASA which has performed inside the ISS [1], [7] and the FEDORE which was sent to ISS by ROSCOSMOS. In this paper, the control architecture, controller tuning and stability analysis of the robotic arms of a Half Humanoid (HH) developed as a precursor for human operations inside a low earth orbital module is presented. The HH is configured with an upper torso, dual arms and an expressive prosthetic face. Lower body has been dispensed off, since it serves no significant purpose for mobility in micro-gravity.

Micro-gravity is typically characterised by one thousand to one ten-millionth of normal earth gravity [6]. Micro-gravity influences the motion of the robotic arm inside the orbital module. Hence the controllers must be tuned to ensure desired performance of the arm in micro-gravity. There are various ways of simulating micro-gravity on earth [5]. However these are costly and are hence not suitable during the tuning phase which involves repeated iterations. One of the alternate approaches could be to use model based tuning. However, in this method accurate modelling of the actuator dynamics is important as it influences the control effort applied to the arm. This is often not possible when off the shelf actuators with built in digital controllers are used as in this case. In this

wake, the paper discusses a hardware based tuning method using the conventional step and frequency response for the actuators in a simulated micro-g orientation. The paper is organised as follows. The kinematic configuration of the half humanoid robotic arm is discussed in section 2 followed by the control architecture in section 3. Section 4 discusses the strategy for controller gain tuning for microgravity operation. The hardware results and analysis are presented in section 5.

II. CONFIGURATION OF THE ROBOTIC ARM OF THE HALF HUMANOID

The half humanoid is anthropomorphically designed with 35 DOF with dual robotic arms each consisting of 6 DOF. The joint axis of the first three joints of each arm are co-incident and mutually perpendicular. All the joints are revolute and the kinematic configuration of the arm is as shown in the Fig. 1. Maximum reach of the arm is 730mm. Modified DH parameters have been used to derive the kinematic model of the arm. Unlike other space robots, the HH is sedentary and attached to the crew seat assembly.

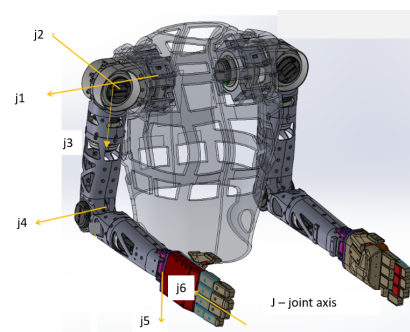


Fig. 1: Kinematic configuration of HH arm

A. Workspace of the arm

The joint excursions of the HH arm joints are limited to match the ranges of motion of human arm. Additionally the workspace of the arm is constrained by virtue of its position inside the orbital module, to avoid collisions of the arm with other mounting structures within the orbital module.

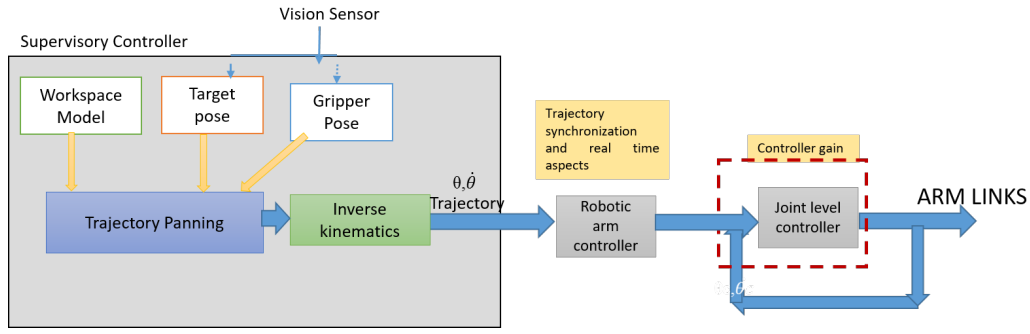


Fig. 2: Control architecture of HH

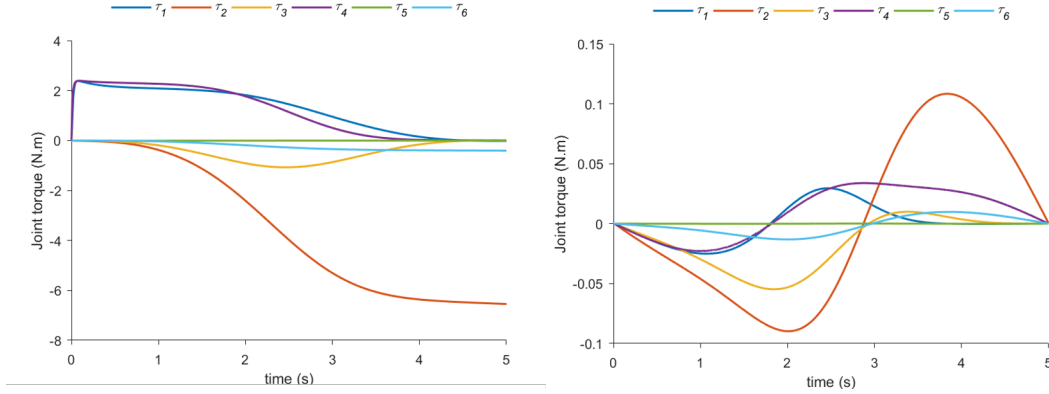


Fig. 3: Comparison of demanded torque in 1-g and 0-g

B. Functionalities of the HH

The HH has been configured to work as a robotic assistant in LEO missions. In the first flight, it would serve as a precursor to the actual manned mission, in which the various robotics technologies necessary for a robotic assistant would be demonstrated and tested. The arm would be used to reach the panel in front of the humanoid and would operate switches, perform gestures and can be positioned to any point in the workspace of the arm in different modes, namely

(i) Joint mode : command each joint to any desired angular position, (ii) Cartesian co-ordinate mode : command the end effector to reach and attain any desired 6D pose in world space, (iii) Trajectory mode : command the arm to follow any desired trajectory consisting of a train of position and velocity commands for each joint, (iv) Straight path mode : command the end effector to follow a straight line motion in task space. The different modes of operation of the arm have been implemented leveraging the MoveIt motion planning pipeline of Robot Operating System (ROS) 1.0.

On the task level, the arm is also able to execute the following control modes.

1) *Visual servoing*: : To overcome the launch induced errors in the calibrated robot, visual servoing algorithm is used which drives the robotic arm in such a way as to match desired pose to the actual pose, both derived from

visual fiducial markers. Conventional visual servoing methods require an obstacle-free path. In our implementation, we have eliminated this requirement by leveraging the obstacle-aware path planning pipeline of ROS MoveIt along with the visual servoing. The scheme was implemented in a robotic arm in ground with artificially introduced joint offsets, simulating launch stress. The worst case error values were within 5 mm and 0.1 rad as against 15 mm and 0.3 rad in open loop. For more details, the reader is referred to [3]

2) *Compliance control*: : To protect the arm against launch vibrations, arm has to be locked. This is akin to the peg-in-hole problem which calls for compliance control. The scheme is implemented and integrated into the existing ROS motion planning pipeline. To test the scheme, deliberate errors were introduced in the initial position. It is seen that for initial errors in position to the tune of 2.5cm and rotation to the tune of approx. 0.122radian is absorbed by the compliance control and the arm is brought within the specified error tolerance of $\leq 2.5\text{mm}$ in position and orientation of $\leq 0.05\text{radian}$.

III. CONTROL ARCHITECTURE

A decentralised control architecture is followed for the HH. This decouples the actuator dynamics from the dynamic motion planning of the entire arm where the planning need not account for the actuator dynamics. The actuator dynamics are then suitably compensated by a joint level servo loop.

The control architecture is as shown in Fig. 2. A central master controller does the motion planning for the arm in its workspace, in the presence of obstacles and within specified joint limits and accelerations. The joint space trajectory thus generated is sent to the individual joint level controllers via the robotic arm controller (RAC). The RAC is used to convert the non-real time trajectory signals received from ROS in real time and to synchronise the motion of the joints. For further details on RAC, reader is referred to [9].

1) *Joint configuration*: Each joint is powered by a embedded actuator with controller, gear, harmonic drive, position encoders and torque sensors. A closed loop position servo loop with tune-able gains is resident in each of the joint actuator. For a varying inertia system such as the HH arms, the high gear ratio ensures that the reflected inertia on the motor side is much lesser and equal to $\frac{J}{n^2}$, where J is the load inertia and n is the gear ratio [2].

IV. PERFORMANCE SPECIFICATIONS FOR THE HH ARM

The half humanoid arm is designed to work with the speed and accuracy of human beings. The targeted end effector position accuracy is ± 1 mm. Through Monte Carlo simulations for random variations, it is found that a joint level accuracy of 0.08 degree is required to achieve this accuracy at the end effector level for the HH. Structural frequency of 12Hz is estimated for the Arm in extended position, hence the bandwidth possible for each joint has to be kept ≤ 6 Hz to avoid control-structure interactions.

V. STRATEGY FOR CONTROLLER GAIN TUNING IN MICROGRAVITY

A. Drawback of model based controller tuning

In micro-gravity environment, the effects of actuator dynamics such as friction effects are more pronounced and as found in [4], it is found to have detrimental effects. Hence a high reliable model incorporating actuator dynamics is necessary for model based tuning of the controller. However, available friction models, such as Lu Gre model, though used extensively in literature, is not sufficient to capture the effects of friction in micro-gravity. Also in cases where the commercial off the shelf components are used for the actuators, it is not often possible to develop a reliable model of the actuator. All this calls for hardware based tuning in microgravity conditions as a promising alternative.

The exorbitant costs of the micro-gravity test platforms inhibit their usage for iterative tuning of gains. The paper proposes a suitable method for repeated iterations in laboratory set up, to design and establish the margins for the individual joint controllers within the workspace, in micro-gravity conditions. The results are further corroborated with testing in planar air bearing test facility.

B. Simulating micro-gravity conditions for arm movement

Gravity acts as an additional load on the motor and varies with position as long as the gravity vector is not along the

rotation axis of the motor. Hence the torque demand in 1g condition will be more than the micro-gravity conditions. The results from the inverse dynamics model of the arm showing the demanded torque at each joint for 1g and 0-g condition for an angular excursion of 0 to 90 deg is as shown in Fig. 3. To simulate micro-gravity under the influence of earth's gravity, it is proposed to mount the joints in such a way that the rotation axis of the joint actuator is aligned along the gravity vector such that gravity no longer appears as load on the joint. Even if the link CG is at an offset from the axis of rotation, resulting load will be taken up by the radial bearings of the motor and not demanded from the motor torque. Hence this is a suitable configuration for simulating micro-gravity. To prove the sufficiency of the set up, joints j2 and j4 are mounted in micro-g orientation with axes along the direction of gravity and the joint torque demands are obtained for an angular excursion from 0 to 90 deg. This is compared with the equivalent results for 1g condition as seen in Fig. ?? In Fig. 4, j2 and j4 execute an excursion of 0 to 90 deg in micro-gravity orientation while j3 and j1 are not in micro-g orientation and hold their position. Joint positions have been given separate axes for legibility while torque is to be read against the axes of the graph. It is seen that for the same range of motion in 1g and the proposed simulated micro-g condition, the torque demand in micro-g is ≤ 0.5 Nm while that in 1g is 3.5 Nm. The lesser torque demanded in micro-g orientation establishes that gravity offloading has happened in the proposed set up. This establishes the sufficiency of such a set up for evaluating performance in micro-gravity.

To use this method effectively, it is necessary that we are able to identify such orientation for each joint of the arm. The micro-g locations selected for the HH arm are as shown in figure 5 which ensures gravity off-loading for all the joints.

C. Dynamic performance

The micro-g orientation set up is sufficient for static tests. However, it needs to be ascertained if the dynamic performance shows variation between 1g and micro-g. For this purpose, a single actuator with simulated inertia load was mounted in both the orientations and torque profiles obtained for both cases individually, as the load executes one complete revolution at a constant velocity of 5 deg/s. An FFT analysis of the torque profiles were done and as seen from Fig. 6a and Fig. 6b, the dominant frequency component is 17.7 Hz which is corresponding to the velocity of movement for a gear ratio of 160 and 8 strain gauge cycles/revolution, thus implying that no other components are introduced during dynamic movement in micro-g.

VI. RESULTS AND ANALYSIS

With the sufficiency of the micro-g orientation set-up established, the step response at various representative locations to account for varying inertia of the arm in the workspace, were taken to tune the PID gains for individual joints. It was seen

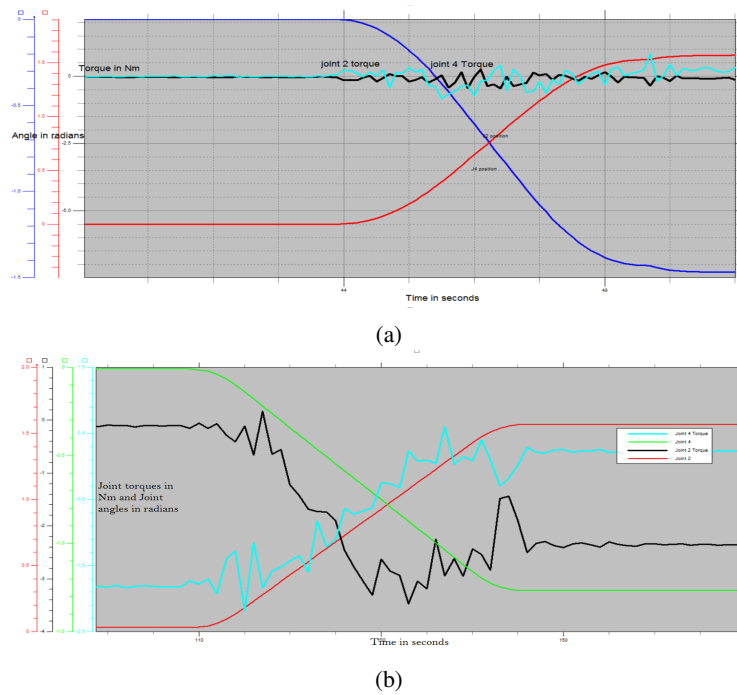


Fig. 4: Joint torques obtained for j2 and j4 (a) zero-g condition and (b) 1-g condition

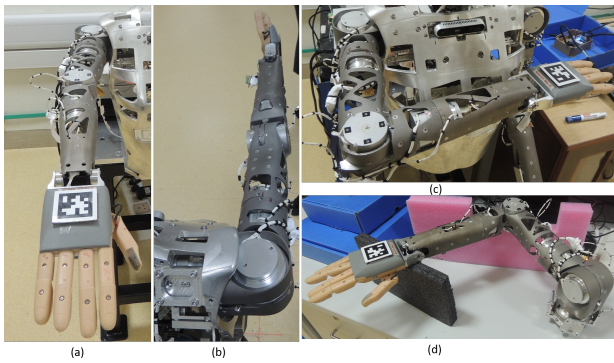
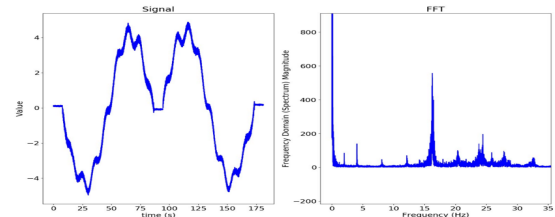
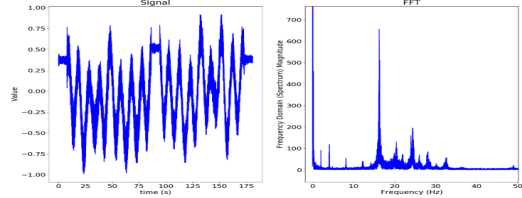


Fig. 5: micro-g mounting configurations of the HH arm (a) joints 2,3,4 and 5 in micro-g orientation (b) joints 2,3 and 5 in micro-g orientation (c) joints 2,4,5 and 6 in micro-g orientation (d) joint 1 in micro-g orientation

that step response displayed steady state error which could be attributed to the effect of friction. Thus an integral gain was introduced to obtain the joint position within 0.08 deg of the commanded position. Once the gain tuning of the individual controllers were done, frequency response of the joints were taken. This was done by keeping the entire arm in position hold mode at representative locations and exciting the joint of interest with sinusoidal commands. The resulting encoder readings were measured and the frequency response was generated. However, since off the shelf actuator was used, closed loop frequency response was obtained in this manner.



(a) for 1g condition



(b) for 0g condition

Fig. 6: FFT of torque signal of a typical joint

Using the well known closed loop transfer function equation

$$CLTF = \frac{G(s)}{1 + G(s)H(s)} \quad (1)$$

and assuming unity feedback, the open loop transfer function is also obtained, which helped establish the relative stability margins of the individual joints. Step response at the extended arm position is the maximum inertia location as shown in Fig.7. Closed loop response showing the bandwidth and open loop response showing the relative stability margins for the

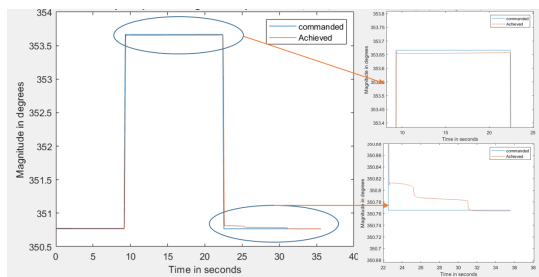


Fig. 7: Step response of joint 2

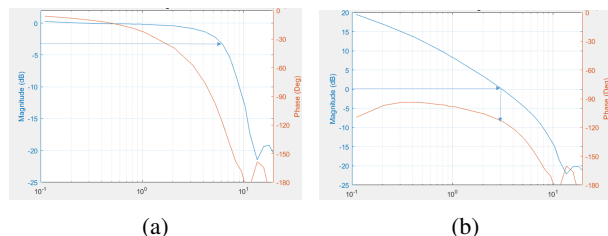


Fig. 8: Frequency response plots for joint 2 (a) closed loop frequency response (b) open loop frequency response

same orientation are shown in Fig. 8. The joint servo loop has a bandwidth of 6Hz, Gain margin of $\geq 15dB$ and phase margin of 70 deg. With the gains tuned using the above procedure, the arm assembly was subjected to performance tests in a planar air bearing as shown in Fig. 9 for verification. The performance of the arm was found to be matching and within specifications. In summary, the paper puts forth a reliable method for iterative tuning of gains using simulated microgravity condition and has verified the results in an actual planar air bearing set up.

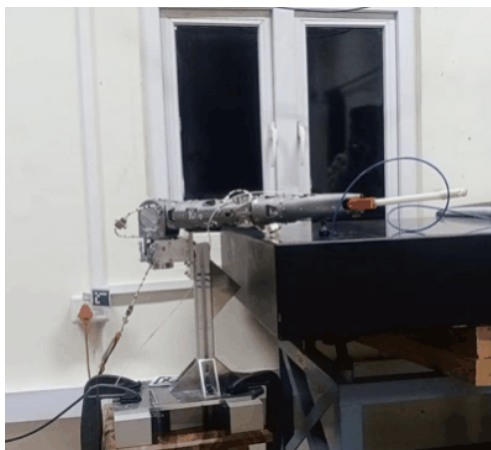


Fig. 9: Performance tests in air bearing facility

REFERENCES

- [1] T.D. Ahlstrom, M.A Diftler et al "Robonaut 2 on the International Space Station: Status Update and Preparations for IVA Mobility", AIAA
- [2] C. Dario, G. A. Magnani, P. Rocco and A. Rusconi, "Position/Torque control of a space robotic arm" Proc. of IFAC 2006.
- [3] H. Ganesan, G. R. Sangeetha and R. Durairaj "On achieving accurate operations in task-space without in-situ kinematic calibration for on-orbit humanoid robotic arms", Frontiers of Aerospace Systems and Technologies, Vikram Sarabhai Space Centre, FAST-2022.
- [4] W. S. Newman, G. D. Glosser, J. H. Miller and D. Rohn, "The detrimental effect of friction on space microgravity robotics," Proceedings 1992 IEEE International Conference on Robotics and Automation, Nice, France, 1992, pp. 1436-1441 vol.2, doi: 10.1109/ROBOT.1992.220149.
- [5] Thomas, V.A. Prasad, N.S. Reddy, C.A.M.. (2000). Microgravity research platforms - A study. Current science. 79. 336-340.
- [6] Microgravity-A Teacher's Guide with Activities in Science, Mathematics, and Technology, EG-1997-08-110-HQ, Education Standards
- [7] Diftler, Myron Mehling, Joshua Abdallah, Muhammad Radford, Nicolaus Bridgwater, Lyndon Sanders, Adam Askew, Roger Linn, D. Yamokoski, John Permenter, Frank Hargrave, Brian Platt, Robert Savely, Robert Ambrose, Robert. (2011). Robonaut 2 - The first humanoid robot in space. Proceedings - IEEE International Conference on Robotics and Automation. 2178-2183. 10.1109/ICRA.2011.5979830.
- [8] Sasiadek, J.. (2014). Space robotics - Present and past challenges. 2014 19th International Conference on Methods and Models in Automation and Robotics, MMAR 2014. 926-929. 10.1109/MMAR.2014.6957481.
- [9] Anwar Backer, Deepa Sara et al."A Decentralized Approach based Embedded System for Trajectory Commanding in Half Humanoid", National Conference on Artificial Intelligence (AI) Enabled Aerobots and Hydrobots, Vikram Sarabhai Space Centre, ASET 2022"